Heteronuclear Hexaplatinum Cluster Complexes: Structure as a Function of Electron Count

Greg J. Spivak, Jagadese J. Vittal, and Richard J. Puddephatt*

Department of Chemistry, University of Western Ontario, London, Canada N6A 5B7

Received May 15, 1998

The 84-electron hexaplatinum cluster complex $[Pt_6(\mu\text{-}CO)_6(\mu\text{-}dppm)_3]$, **1**, dppm = $Ph_2PCH_2PPh_2$, reacts in a 1:2 molar ratio with either 0-electron metalloligands LM^+ (L = Ph_3P, M = Cu, Ag, Au; L = *i*Pr_3P, M = Au) or InX_3 (X = Cl, Br) or 2-electron metalloligands Tl^+ and Hg to give the corresponding 84-electron clusters $[Pt_6(\mu_3\text{-}ML)_2(\mu\text{-}CO)_6(\mu\text{-}dppm)_3]^{2+}$ or $[Pt_6(\mu_3\text{-}InX_3)_2(\mu\text{-}CO)_6(\mu\text{-}dppm)_3]$ or 88-electron clusters $[Pt_6(\mu_3\text{-}Tl)_2(\mu\text{-}CO)_6(\mu\text{-}dppm)_3]^{2+}$ and $[Pt_6(\mu_3\text{-}Hg)_2(\mu\text{-}CO)_6(\mu\text{-}dppm)_3]$, respectively. The mercury cluster is oxidized by CH_2I_2 to give the known 86-electron cluster $[Pt_6(\mu_3\text{-}HgI)_2(\mu\text{-}CO)_6(\mu\text{-}dppm)_3]$. Reaction of **1** with $[Ir(CO)_4]^-$ occurs in a 1:1 ratio only to give the 98-electron anionic cluster $[Pt_6\{\mu_3\text{-}Ir(CO)_2\}(\mu\text{-}CO)_6(\mu\text{-}dppm)_3]^-$, which reacts with $[Ph_3PAu]^+$ to give $[Pt_6\{\mu_3\text{-}Ir(CO)_2\}(\mu_3\text{-}AuPPh_3)(\mu\text{-}CO)_6(\mu\text{-}dppm)_3]$. The new cluster complexes are characterized by NMR and IR spectroscopies, and $[Pt_6(\mu_3\text{-}AuP\textit{i}Pr_3)_2(\mu\text{-}CO)_6(\mu\text{-}dppm)_3]^{2+}$ is also characterizedby an X-ray structure determination.

Introduction

The study of heteronuclear clusters of the platinum group metals continues to yield interesting new structures which are of interest both in understanding cluster structure as a function of electron count and in modeling metal−metal interactions in the bimetallic catalysts used in petroleum re-forming.[1] In particular, the triangular Pt_3 unit in trinuclear platinum clusters has proven to be a versatile building block for the formation of larger, heteronuclear platinum clusters by reaction with many main group metal and transition metal reagents.[1,2] For example, the $Pt_3(\mu\text{-}dppm)_3$ cluster building block, dppm = $Ph_2PCH_2PPh_2$, which is present in the cationic clusters $[Pt_3(\mu_3\text{-}CO)(\mu\text{-}dppm)_3]^{2+}$ and $[Pt_3(\mu_3\text{-}H)(\mu\text{-}dppm)_3]^+$ can add electrophilic gold fragments $[AuPR_3]^+$ (PR_3 = tertiary phosphine) to yield $[Pt_3(\mu_3\text{-}AuL)_n(\mu\text{-}dppm)_3]^{n+}$ (n = 1, 2) or nucleophilic Hg(0) to yield $[Pt_3(\mu_3\text{-}Hg)_2(\mu\text{-}dppm)_3]^{2+}$.[3] Similar reactivity is observed for the Chatt−Chini clusters $[Pt_3(\mu\text{-}CO)_3(PR_3)_n]$ (n = 3, 4), which react with both electrophilic $[AuPR_3]^+$ and nucleophilic reagents such as Hg(0) or Tl(I) to yield $[Pt_3(\mu_3\text{-}MPR_3)(\mu\text{-}CO)_3(PR_3)_n]^+$ and $[Pt_3(\mu_3\text{-}L)(\mu\text{-}CO)_3(PR_3)_3]^{m+}$ (L = Hg, m = 0; L = Tl, m = 1), respectively.[4,5]

This article describes efforts to develop a related chemistry of hexaplatinum clusters, and the background research is outlined below (Scheme 1). The enabling discovery was the synthesis of a suitable precursor cluster, the 84-electron $[Pt_6(\mu\text{-}CO)_6(\mu\text{-}dppm)_3]$, **1**, which contains two $\{Pt_3(\mu\text{-}CO)_3\}$ units held together by three bridging dppm ligands, and thus has 2

Scheme 1

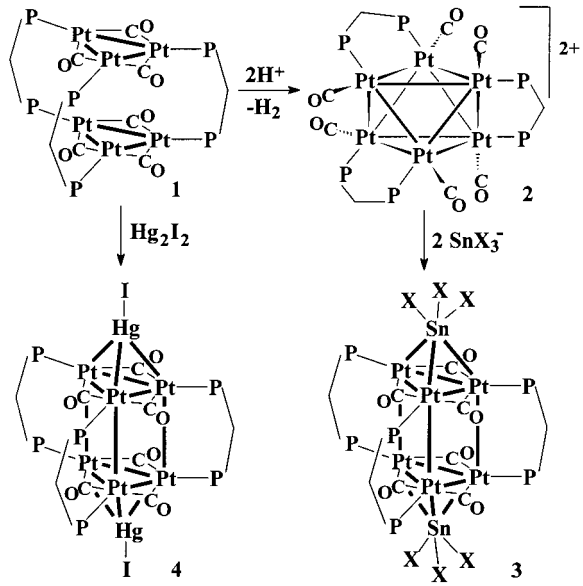

(1) (a) Adams, R. D., Ed. *Comprehensive Organometallic Chemistry II*; Pergamon: Oxford, U.K., 1995; Vol. 10. (b) Braunstein, P.; Rose, J. In Catalysis by Di- and Polynuclear Metal Clusters; Adams, R. D., Cotton, F. A., Eds.; Wiley: New York, 1997; p 346. (c) Xiao, J.; Puddephatt, R. J. *Coord. Chem. Rev.* **1995**, *143*, 457.

(2) (a) Imhof, D.; Venanzi, L. M. *Chem. Soc. Rev.* **1994**, *23*, 185. (b) Burrows, A. D.; Mingos, D. M. P. *Coord. Chem. Rev.* **1996**, *154*, 19. (c) Puddephatt, R. J.; Manojlovic-Muir, Lj.; Muir, K. W. *Polyhedron* **1990**, *9*, 2767.

(3) (a) Ramachandran, R.; Payne, N. C.; Puddephatt, R. J. *J. Chem. Soc., Chem. Commun.* **1989**, 128. (b) Payne, N. C.; Ramachandran, R.; Schoettel, G.; Vittal, J. J.; Puddephatt, R. J. *Inorg. Chem.* **1991**, *30*, 4048. (c) Schoettel, G.; Vittal, J. J.; Puddephatt, R. J. *J. Am. Chem. Soc.* **1990**, *112*, 6400.

(4) (a) Briant, C. E.; Wardle, R. W. M.; Mingos, D. M. P. *J. Organomet. Chem.* **1984**, *267*, C49. (b) Mingos, D. M. P.; Wardle, R. W. M. *J. Chem. Soc., Dalton Trans.* **1986**, 73. (c) Mingos, D. M. P.; Oster, P.; Sherman, D. J. *J. Organomet. Chem.* **1987**, *320*, 257. (d) Bour, J. J.; Kanters, R. P. E.; Schlebos, P. P. J.; Bos, W.; Bosman, W. P.; Behm, H.; Beurskens, P. T.; Steggerda, J. J. *J. Organomet. Chem.* **1987**, *329*, 405. (e) Hill, C. M.; Mingos, D. M. P.; Powell, H.; Watson, M. J. *J. Organomet. Chem.* **1992**, *441*, 499. (f) Imhof, D.; Burckhardt, U.; Dahmen, K.-H.; Ruegger, H.; Gerfin, T.; Gramlich, V. *Inorg. Chem.* **1993**, *32*, 5206. (g) Imhof, D.; Burckhardt, U.; Dahmen, K.-H.; Joho, F.; Nesper, R. *Inorg. Chem.* **1997**, *36*, 1813.

(5) (a) Ezomo, O. J.; Mingos, D. M. P.; Williams, I. D. *J. Chem. Soc., Chem. Commun.* **1987**, 924. (b) Albinati, A.; Moor, A.; Pregosin, P. S.; Venanzi, L. M. *J. Am. Chem. Soc.* **1982**, *104*, 7672.

10.1021/ic980555j CCC: $15.00 © 1998 American Chemical Society
Published on Web 09/24/1998

× triangular stereochemistry.[6] Thus each $\{Pt_3(\mu\text{-}CO)_3P_3\}$ unit in **1** is analogous to a Chatt-Chini cluster $[Pt_3(\mu\text{-}CO)_3(PR_3)_3]$ and it is likely that intertriangle Pt···Pt bonding is weak or absent. Oxidation of cluster **1** occurs easily and reversibly to give the cationic 82-electron cluster $[Pt_6(CO)_6(\mu\text{-dppm})_3]^{2+}$, **2**, which contains a distorted octahedral Pt_6 core,[6] and the change in geometry as a function of electron count is consistent with the predictions of the polyhedral skeletal electron pair theory (PSEPT) modified for platinum clusters.[7] Cluster **1** also adds one phosphite or alkyne ligand to give the corresponding 86-electron cluster $[Pt_6(\mu\text{-}CO)_6(\mu\text{-dppm})_3L]$, L = phosphite or alkyne, which undergoes easy cluster fragmentation.[8] More stable, heteronuclear 86-electron Pt_6 clusters have been prepared either by the addition of two 2-electron ligands such as $[SnX_3]^-$ (X = halide) to **2** to yield the clusters $[Pt_6(\mu_3\text{-}SnX_3)_2(\mu\text{-}CO)_6(\mu\text{-dppm})_3]$, **3**,[8] or by the addition of two 1-electron ligand fragments, derived from simple reagents such as Hg_2X_2 (X = halide), to **1** to yield the clusters $[Pt_6(\mu_3\text{-}HgX)_2(\mu\text{-}CO)_6(\mu\text{-dppm})_3]$, **4**.[8] This novel reaction was termed a *bicluster* oxidative addition reaction. The Pt_6 cores in both **3** and **4** adopt a trigonal prismatic stereochemistry, consistent with that found for the anionic cluster $[Pt_6(\mu\text{-}CO)_6(CO)_6]^{2-}$, which also has an 86-electron count.[9] Thus, either increasing or decreasing the electron count from 84 electrons leads to increased Pt−Pt bonding, but the 82-electron and 86-electron clusters have fundamentally different core structures.[8] This paper extends these studies by addition of either 0-electron or 2-electron ligands to complex **1** to give heteronuclear clusters with Pt_6M_2 cores having 84-, 86-, or 88-electron counts.

Results

Synthesis of the New Heteronuclear Pt_6 Clusters. The synthesis of heteronuclear 84-electron Pt_6M_2 clusters from **1** is shown in Scheme 2. Thus, the clusters $[Pt_6(\mu_3\text{-}MPR_3)_2(\mu\text{-}CO)_6(\mu\text{-dppm})_3][PF_6]_2$, **5** (R = Ph: M = Au, **5a**; M = Ag, **5b**; M = Cu, **5c**. R = *i*Pr: M = Au, **5d**) were isolated as dark green solids from tetrahydrofuran (THF) solutions containing **1** and 2 equivs of the corresponding reagent $[M(THF)(PR_3)][PF_6]$ in good yields. The clusters **5** were only slowly decomposed in moist air when M = Cu or Au, but the silver derivative **5b** proved to be extremely sensitive to both air and light. This relative stability series for **5** of M = Au > Ag < Cu is consistent with previous work on heteronuclear platinum clusters containing coinage metals.[4g] In a similar synthetic method, the addition of 2 equivs of InX_3 (X = halide) to a THF solution of cluster **1** caused an immediate color change from purple to either brown (X = Cl) or red-brown (X = Br), and the products $[Pt_6(\mu_3\text{-}InX_3)_2(\mu\text{-}CO)_6(\mu\text{-dppm})_3]$, **6** (X = Cl, **6a**; X = Br, **6b**), were isolated in good yields (Scheme 2). Note that the electron count used is for the Pt_6 unit only, counting either the $[MPR_3]^+$ or InX_3 units as 0-electron ligands. This is appropriate since the similarity in structures of the Pt_6 cores in **5** and **6** is then emphasized, but it is of course also possible to consider the adducts as octanuclear clusters and then **5** and **6** are not strictly isoelectronic.[7]

Scheme 2

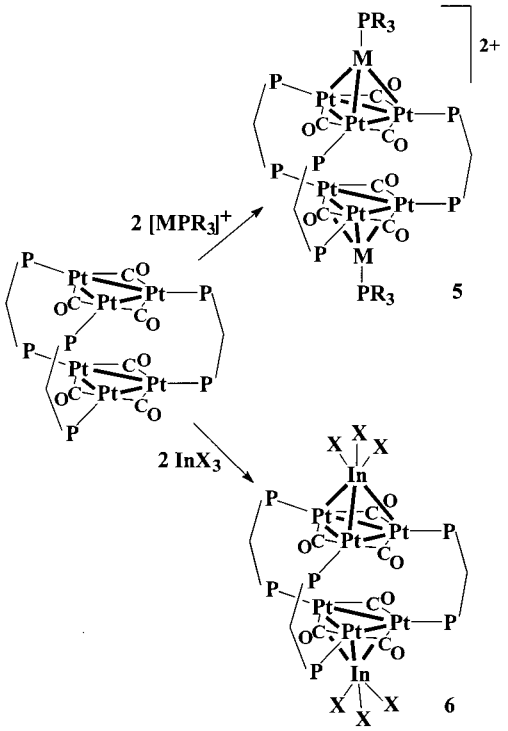

Scheme 3

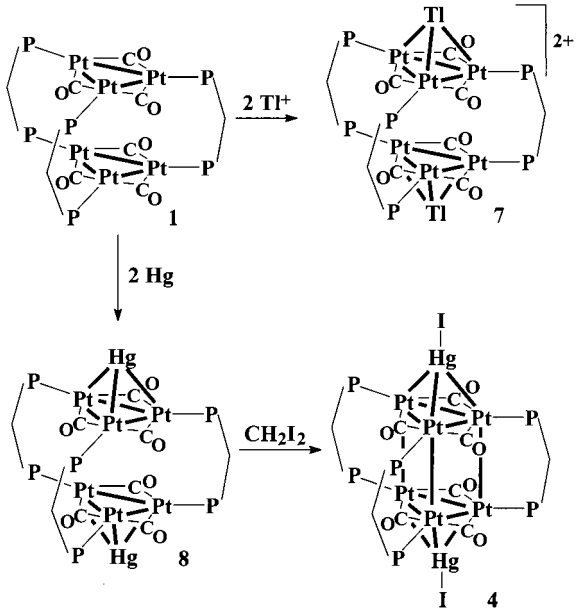

The formation of 88-electron clusters by reaction of **1** with the ligands Tl^+ and Hg is summarized in Scheme 3. Both Tl^+ and Hg can be considered as 2-electron donor ligands using their $6s^2$ electrons.[5b] The adducts with **1** have very intense colors. Thus, the addition of 2 equivs of $TlPF_6$ to a THF solution of cluster **1** causes a color change from dark purple to dark blue and yields a dark blue solid after workup. Similarly, when a THF solution of **1** is treated with an excess of elemental mercury, the solution turns deep, dark blue-green and a solid of the same color is isolated in good yield. Unfortunately, crystals suitable for an X-ray crystal structure determination

(6) Hao, L.; Spivak, G. J.; Xiao, J.; Vittal, J. J.; Puddephatt, R. J. *J. Am. Chem. Soc.* **1995**, *117*, 7011.
(7) (a) Mingos, D. M. P.; May, A. S. In *The Chemistry of Metal Cluster Complexes;* Shriver, D. F., Kaesz, H. D., Adams, R. D., Eds.; VCH: New York, 1990. (b) Mingos, D. M. P.; Wales, D. J. *Introduction to Cluster Chemistry*; Prentice Hall: Englewood Cliffs, NJ, 1990; Chapter 2.
(8) (a) Spivak, G. J.; Hao, L.; Vittal, J. J.; Puddephatt, R. J. *J. Am. Chem. Soc.* **1996**, *118*, 225. (b) Spivak, G. J.; Manojlovic-Muir, Lj.; Muir, K. W.; Puddephatt, R. J.; Hao, L.; Vittal, J. J.; Dmitrii, Y. *Inorg. Chim. Acta* **1997**, *265*, 65. (c) Spivak, G. J.; Puddephatt, R. J. *Inorg. Chim. Acta* **1997**, *264*, 1. (d) Spivak, G. J.; Puddephatt, R. J. *J. Organomet. Chem.*, in press.
(9) Calabrese, J. C.; Dahl, L. F.; Chini, P.; Longoni, G.; Martinengo, S. *J. Am. Chem. Soc.* **1974**, *96*, 2614.

Scheme 4

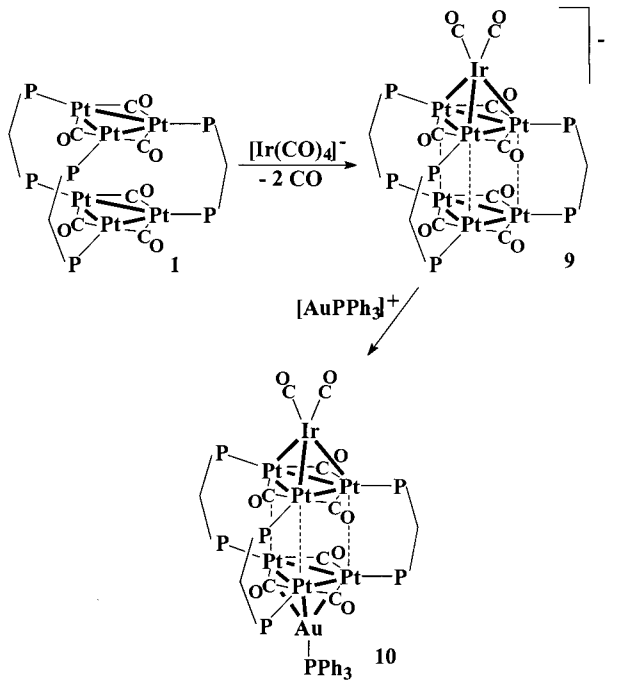

could not be obtained in either case. However, microanalyses and spectroscopic data had established that both products correspond to 1:2 adducts of the starting material **1** and of $TlPF_6$ and Hg, respectively, and are characterized spectroscopically as $[Pt_6(\mu_3\text{-}Tl)_2(\mu\text{-}CO)_6(\mu\text{-}dppm)_3][PF_6]_2$, **7**, and $[Pt_6(\mu_3\text{-}Hg)_2(\mu\text{-}CO)_6(\mu\text{-}dppm)_3]$, **8**. Cluster **8** reacts with excess CH_2I_2 and yields the known cluster $[Pt_6(\mu_3\text{-}HgI)_2(\mu\text{-}CO)_6(\mu\text{-}dppm)_3]$,[8] as determined by $^{31}P\{^1H\}$ and ^1H NMR spectroscopy (Scheme 3).

The reaction of **1** with [PPN][$Ir(CO)_4$], PPN = $(Ph_3P)_2N^+$, is shown in Scheme 4. In this case, the reagent acts as a source of $\{Ir(CO)_2\}^-$ but only one such unit adds to **1** even in the presence of excess [PPN][$Ir(CO)_4$]. The product **9** is stable in solution at room temperature for several hours under nitrogen, but it is extremely air-sensitive. The primary platinum-containing decomposition product is **1**, as determined by NMR, but the fate of the $Ir(CO)_2^-$ fragment has not been determined. If $\{Ir(CO)_2\}^-$ is considered as a 2-electron ligand, then the formation of **9** can be compared to the addition of a single phosphite ligand to **1** to give an 86-electron cluster rather than to the addition of two units of Hg(0) to give the 88-electron cluster **8**. The difference probably arises from the much greater donor strength of $Ir(CO)_2^-$ compared to Hg(0), such that addition to one Pt_3 face of **1** leads to partial transfer of negative charge to the second Pt_3 face, which is therefore deactivated toward attack by a second nucleophile.[8c] If this is so, it seemed likely that the second face would be activated toward electrophilic attack, and indeed, **9** did form an adduct with $\{AuL\}^+$ formulated as $[Pt_6\{\mu_3\text{-}Ir(CO)_2\}(\mu_3\text{-}AuPPh_3)(\mu\text{-}CO)_6(\mu\text{-}dppm)_3]$, **10**, which has much greater stability to air than **9**. Clusters **9** and **10** are deep red and red-brown, respectively, and they represent rare examples of heteronuclear PtIr clusters.[10]

Structure of 5d. Recrystallization of cluster **5d** from diethyl ether/CH_2Cl_2 yielded crystals of the mixed chloride−hexafluorophosphate salt $[Pt_6(\mu_3\text{-}AuPiPr_3)_2(\mu\text{-}CO)_6(\mu\text{-}dppm)_3][Cl][PF_6]$, whose structure was determined crystallographically. It is assumed that the chloride is derived from the recrystallization solvent. There are two independent cluster cations **5d** in each unit cell, but the structures are very similar; the structure of one of them is shown in Figure 1, and selected bond distances and angles are listed in Table 1. Each molecule of **5d** has approximately D_{3h} symmetry with a distorted trigonal prismatic Pt_6 core in which each triangular face is capped by a triply bridging $AuPiPr_3$ group. In each molecule, the μ-CO ligands bridge each edge of the Pt_3 triangles and the dppm ligands bridge between pairs of platinum atoms on adjacent Pt_3 triangles. The dppm phosphorus atoms and the CO ligands are roughly coplanar with each Pt_3 unit. The range of intratriangle Pt−Pt distances [2.670(2)−2.734(2) Å] in **5d** is similar to those found in other structurally characterized clusters containing a $\{Pt_3(\mu_3\text{-}AuPR_3)\}$ unit, such as $[Pt_3(\mu_3\text{-}AuPCy_3)(\mu\text{-}CO)_3(PCy_3)_3]^+$ [2.678(5)−2.705(6) Å],[4a] $[Pt_3(\mu_3\text{-}AuPCy_3)(\mu\text{-}CO)_2(\mu\text{-}SO_2)(PCy_3)_3]^+$ [2.667(4)−2.746(1) Å],[4b] $[Pt_3(\mu_3\text{-}AuPPh_3)(\mu\text{-}CO)_3(PPh_3)_4]^+$ [2.666(1)−2.708(1) Å],[4d] and $[\{Pt_3(\mu\text{-}CO)_3(PCy_3)_3\}_2\{(AuPPh_2)_2(CH_2)_2C_6H_4\}]^{2+}$ [2.6627(8)−2.6701(13) Å].[4g] Also, these distances are only slightly longer than those found in the

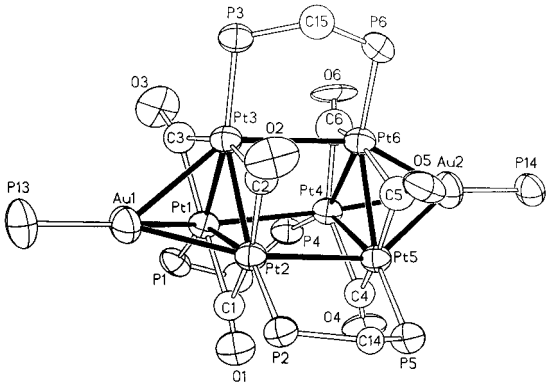

Figure 1. View of one of the two independent cluster cations $[Pt_6(\mu_3\text{-}AuPiPr_3)_2(\mu\text{-}CO)_6(\mu\text{-}dppm)_3]^{2+}$.

Table 1. Selected Bond Distances and Torsion Angles for Cluster **5d**[a]

Bond Distances (Å)			
Pt(1)−Pt(2)	2.717(2)	Pt(7)−Pt(8)	2.690(2)
Pt(1)−Pt(3)	2.687(2)	Pt(7)−Pt(9)	2.722(2)
Pt(2)−Pt(3)	2.709(2)	Pt(8)−Pt(9)	2.712(2)
Pt(4)−Pt(5)	2.697(2)	Pt(10)−Pt(11)	2.670(2)
Pt(4)−Pt(6)	2.691(2)	Pt(10)−Pt(12)	2.721(2)
Pt(5)−Pt(6)	2.734(2)	Pt(11)−Pt(12)	2.713(2)
Pt(1)−Au(1)	2.792(2)	Pt(7)−Au(3)	2.869(2)
Pt(2)−Au(1)	2.774(2)	Pt(8)−Au(3)	2.786(2)
Pt(3)−Au(1)	2.886(2)	Pt(9)−Au(3)	2.803(2)
Pt(4)−Au(2)	2.918(2)	Pt(10)−Au(4)	2.710(2)
Pt(5)−Au(2)	2.818(2)	Pt(11)−Au(4)	2.949(3)
Pt(6)−Au(2)	2.729(2)	Pt(12)−Au(4)	2.820(2)
Pt(1)−Pt(4)	3.106(2)	Pt(7)−Pt(10)	3.030(2)
Pt(2)−Pt(5)	3.031(2)	Pt(8)−Pt(11)	3.059(2)
Pt(3)−Pt(6)	3.077(2)	Pt(9)−Pt(12)	3.033(2)

Torsion Angles (deg)			
P(1)−Pt(1)−Pt(4)−P(4)	11.7(4)	P(7)−Pt(7)−Pt(10)−P(10)	18.3(4)
P(2)−Pt(2)−Pt(5)−P(5)	7.1(4)	P(8)−Pt(8)−Pt(11)−P(11)	15.2(4)
P(3)−Pt(3)−Pt(6)−P(6)	10.1(3)	P(9)−Pt(9)−Pt(12)−P(12)	6.9(4)
Pt(1)−Pt(2)−Pt(5)−Pt(4)	9.7(1)	Pt(7)−Pt(8)−Pt(11)−Pt(10)	15.7(1)
Pt(3)−Pt(1)−Pt(4)−Pt(6)	8.7(1)	Pt(8)−Pt(9)−Pt(12)−Pt(11)	16.0(1)
Pt(2)−Pt(3)−Pt(6)−Pt(5)	9.5(1)	Pt(7)−Pt(9)−Pt(12)−Pt(10)	15.5(1)

[a] Atom labeling: molecule 1 contains atoms Pt(1)−Pt(6), Au(1)−Au(2), P(1)−P(6), P(13)−P(14), C(1)O(1)−C(6)O(6); molecule 2 contains atoms Pt(7)−Pt(12), Au(3)−Au(4), P(7)−P(12), P(15)−P(16), C(7)O(7)−C(12)O(12).

(10) (a) Farrugia, L. J. *Adv. Organomet. Chem.* **1990**, *31*, 301. (b) Bhaduri, S.; Sharma, K. R.; Clegg, W.; Sheldrick, G. M.; Stalke, D. *J. Chem. Soc., Dalton Trans.* **1984**, 2851. (c) Fumagalli, A.; Pergola, R. D.; Bonacina, F.; Garlaschelli, L.; Moret, M.; Sironi, A. *J. Am. Chem. Soc.* **1989**, *111*, 165. (d) Tanase, T.; Toda, H.; Kobayashi, K.; Yamamoto, Y. *Organometallics* **1996**, *15*, 5272. (e) Spivak, G. J.; Yap, G. P. A.; Puddephatt, R. J. *Polyhedron* **1997**, *16*, 3861.

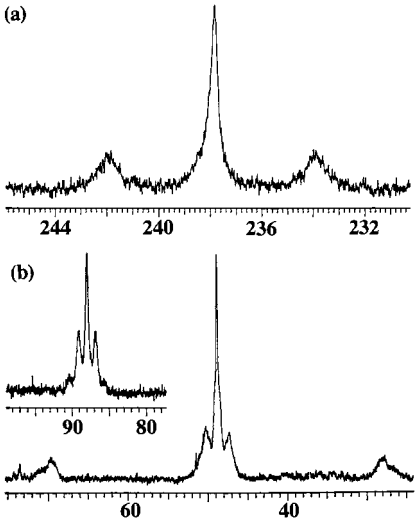

Figure 2. NMR spectra of **5a** in CD_2Cl_2 at −90 °C: (a) ^{13}C NMR spectrum (75.3 MHz) of a ^{13}CO-enriched sample; (b) ^{31}P NMR spectrum (121.4 MHz) showing the dppm resonance and (inset) the PPh_3 resonance.

bicapped Pt_6 clusters **3** [2.656(2)−2.681(2) Å] and **4** [2.634(1)−2.687(1) Å].[8] There is some asymmetry in each $Pt_3(\mu_3$-Au) unit, as indicated by the range of Pt−Au distances [2.710(2)−2.949(3) Å] in **5d**, but all are in the expected range for Pt−Au single bonds.[4] The observed asymmetry most likely arises as a result of steric effects between the dppm phenyl groups and the isopropyl groups of each $[\mu_3$-AuP*i*Pr$_3]^+$ ligand.

The intertriangle Pt−Pt distances in each molecule are long, ranging from 3.031(2) to 3.106(2) Å in one molecule and from 3.030(2) to 3.059(2) Å in the other. These distances in **5d** are significantly longer than those in clusters **3** [2.910(2)−2.948(2) Å] and **4** [2.929(2)−2.946(2) Å] by ca. 30σ. Thus, as expected, intertriangle Pt−Pt bonding is weaker in the 84-electron clusters than in the 86-electron clusters; indeed it is likely that the intertriangle Pt···Pt distances are controlled by the natural bite distance of the bridging dppm ligands in **5d**. The selected torsion angles listed in Table 1 show that the molecular core of **5d** is distorted about the pseudo-C_3 axis by a twist of ca. 10° in one molecule and ca. 15° in the other.

Spectroscopic (IR and NMR) Studies. Clusters **5**−**8** were characterized by variable-temperature $^{13}C\{^1H\}$ and $^{31}P\{^1H\}$ NMR spectroscopy and by IR spectroscopy. The spectroscopic data indicate that they are all isostructural and support each molecule having approximately D_{3h} symmetry.

(a) The 84-Electron Clusters 5 and 6. The resonances in the $^{13}C\{^1H\}$ and $^{31}P\{^1H\}$ NMR spectra of clusters **5a**−**d** at room temperature were very broad, but except for those of **5b**, the peaks sharpened somewhat in the low-temperature (−90 °C) NMR spectra. This broadening at room temperature may arise from reversible fragmentation of the clusters.

The $^{31}P\{^1H\}$ NMR spectra of clusters **5** in CD_2Cl_2 at −90 °C each contained two resonances with satellites due to coupling to ^{195}Pt ($I = {}^1/_2$, 33.8% natural abundance): one signal is due to the bridging dppm ligands and the second to the monophosphine ligands of the μ_3-MPR_3 groups. For example, the $^{31}P\{^1H\}$ NMR spectrum of **5a** shows a somewhat broad resonance at $\delta(^{31}P) = 42.5$, with satellites due to coupling to ^{195}Pt, and is attributed to the six equivalent dppm phosphorus atoms (Figure 2). The ^1J(PtP) coupling constant of 5070 Hz is slightly lower than that measured for the parent cluster **1** [^1J(PtP) = 5289 Hz][6] and those found for the $Pt_6(HgX)_2$ clusters **3** (5127−5257 Hz) and $Pt_6(SnX_3)_2$ clusters **4** (5052−5214 Hz).[8] A second resonance centered at $\delta(^{31}P) = 88.0$ is assigned to the PPh_3 ligand coordinated to gold (Figure 2b, inset). This signal appeared as a 1:4:7:4:1 quintet pattern due to the coupling ^2J(PtAuP), characteristic of a triply bridging $Pt_3(\mu_3$-AuPPh$_3$) group.[2,11] Any coupling between the dppm phosphorus atoms and the PPh_3 phosphorus atoms was too small to resolve. The spectra of **5c** and **5d** were similar, but the spectrum of the less stable silver cluster **5b** was too broad for the ^{195}Pt satellites to be resolved.

Both the IR and low-temperature $^{13}C\{^1H\}$ NMR spectra of clusters **5** clearly showed that the CO ligands are equivalent and bridging.[12] Moreover, the CO absorptions observed for **5a**−**d** are shifted to higher frequencies by ca. 50 cm^{-1} compared to those of cluster **1** [ν(CO) = 1790 (s), 1773 (w) cm^{-1}].[6] For example, the IR spectrum of **5a** showed a strong absorption in the μ-CO region at 1851 cm^{-1} with a weaker signal at 1816 cm^{-1}. This shift is consistent with diminished π-back-bonding from the platinum atoms to the CO ligands as a result of the addition of the electrophilic $[MPR_3]^+$ groups, and the sequence of ν(CO) for M = Cu > Au > Ag may indicate the relative electrophilicities of the corresponding Ph_3PM^+ groups. The $^{13}C\{^1H\}$ NMR spectrum of ^{13}CO-enriched **5a** at −90 °C in CD_2Cl_2 solution contained a single carbonyl resonance at $\delta(^{13}C) = 237.9$, in the region expected for bridging rather than terminal CO ligands (Figure 2).[12] This signal appeared as a five-line multiplet with integrated relative intensities 1:8:18:8:1 due to ^1J(PtC) coupling, as expected for a CO ligand bridging two platinum atoms, but the satellite spectra were broad and the outer peaks were barely resolved. The ^1J(PtC) coupling constant was determined to be 602 Hz, that is 155 Hz lower than that observed for cluster **1** [^1J(PtC) = 757 Hz].[6]

The clusters **6** were conveniently characterized by NMR at room temperature since the broadening effects seen for **5** were not observed. The IR and NMR (23 °C, CD_2Cl_2) data established that all carbonyl and methylene groups and dppm phosphorus atoms are equivalent and that the carbonyl ligands are doubly bridging. Thus, clusters **6** are proposed to have structures in which the InX_3 ligand triply bridges each Pt_3 face in **1**, in a similar manner as the $[MPR_3]^+$ ligands in clusters **5**. When compared to those of **5**, the values of ν(CO) for **6** are higher and the values of ^1J(PtC) are lower, indicating that the InX_3 groups are stronger electrophiles than Ph_3PM^+.

(b) The 88-Electron Clusters 7 and 8. The electron-rich cluster **7** is unstable, and although it can be handled in air for short periods of time, it decomposes after several days even in the absence of air. Cluster **7** has limited solubility in most common organic solvents, and it reacts rapidly with chlorinated solvents to give [$PtCl_2(\eta^2$-dppm)]; it is sufficiently soluble in acetone to give adequate NMR spectra. The $^{31}P\{^1H\}$ and $^{13}C\{^1H\}$ NMR spectra of **7** at room temperature (23 °C) each give singlet resonances with satellites due to coupling to ^{195}Pt and no change in resolution at low temperatures (−90 °C). Coupling to ^{203}Tl and ^{205}Tl (both $I = {}^1/_2$; natural abundances 29.5% and 70.5%, respectively) was not observed. The dppm ^{31}P chemical shift [$\delta(^{31}P) = 46.0$] is comparable to the ^{31}P chemical shifts observed for cluster **1** and clusters **5a**, **5c**, and **5d**, although the ^1J(PtP) coupling of 4813 Hz is unusually low, almost 500 Hz

(11) (a) Lloyd, B. R.; Bradford, A.; Puddephatt, R. J. *Organometallics* **1987**, *6*, 424. (b) Bradford, A.; Jennings, M. C.; Puddephatt, R. J. *Organometallics* **1988**, *7*, 792. (c) Bradford, A. M.; Douglas, G.; Manojlovic-Muir, Lj.; Muir, K. W.; Puddephatt, R. J. *Organometallics* **1990**, *9*, 409. (d) Xiao, J.; Hao, L.; Puddephatt, R. J.; Manojlovic-Muir, Lj.; Muir, K. W.; Torabi, A. A. *Organometallics* **1995**, *14*, 4183. (e) Hao, L.; Xiao, J.; Vittal, J. J.; Puddephatt, R. J.; Manojlovic-Muir, Lj.; Muir, K. W.; Torabi, A. A. *Inorg. Chem.* **1996**, *35*, 658.
(12) Aubke, F.; Wang, C. *Coord. Chem. Rev.* **1994**, *137*, 483.

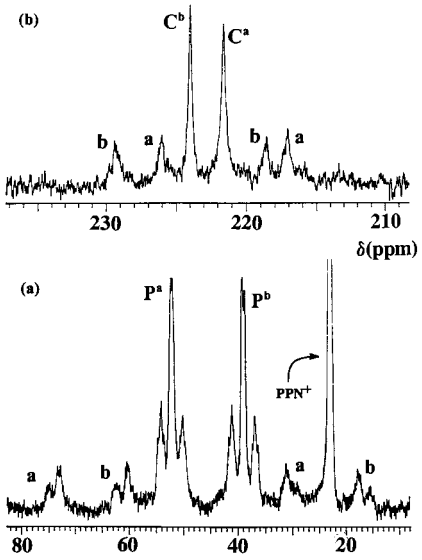

Figure 3. NMR spectra of **9** at −40 °C: (a) ^{31}P NMR spectrum (121.4 MHz); (b) ^{13}C NMR spectrum (75.3 MHz) of a ^{13}CO-enriched sample in the bridging carbonyl region.

lower than for the cluster **1**. The $^{13}C\{^1H\}$ NMR spectrum of ^{13}CO-enriched **7** gave a five-line multiplet centered at $\delta(^{13}C) = 235.4$ with relative intensities 1:8:18:8:1 as expected for bridging CO ligands. The ^1J(PtC) coupling of 733 Hz is large relative to the values for **5** and **6** and is only 24 Hz lower than that for cluster **1**. The IR spectrum of **7** [ν(CO) = 1885 (sh), 1841 (s), 1790 (sh) cm^{-1}] is also consistent with bridging CO ligands, and the ν(CO) values are higher than those observed for cluster **1**, suggesting that the Tl^+ ligand acts as an electrophile overall. Platinum clusters containing triply bridging thallium ligands are not without precedence. Thus, cluster **7** has structural similarities to the crystallographically characterized cluster $[Pt_3(\mu_3\text{-}Tl)(\mu\text{-}CO)_3(PCy_3)_3][Rh(COD)Cl_2]$[5a] and the cluster $[Pt_3\{\mu_3\text{-}Tl(acac)\}(\mu_3\text{-}ReO_3)(\mu\text{-}dppm)_3]^+$,[11] both of which contain a thallium-capped Pt_3 triangle.

Complex **8** was sparingly soluble, and so characterization by NMR was not easy. The $^{31}P\{^1H\}$ NMR spectrum of **8** in CD_2Cl_2 at 23 °C gave a very broad signal at $\delta(^{31}P) = 51.2$ with a ^1J(PtP) coupling of 5600 Hz; this value is the highest value of ^1J(PtP) observed for a Pt_6 cluster. The solubility was too low to give a satisfactory ^{13}C spectrum, even after ^{13}CO enrichment. However, the IR spectrum [ν(CO) = 1843 (m), 1811 (s), 1771 (m) cm^{-1}] clearly indicated the presence of μ-CO ligands. The frequencies are lower than those found for **7** and only slightly higher than those observed for cluster **1**. Thus, as expected, Hg(0) is less electrophilic than Tl(I).

(c) The 86-Electron Clusters 9 and 10. The NMR spectra of **9** were best resolved at −40 °C, with broadening at both higher and lower temperatures. The ^{31}P NMR spectrum (Figure 3) contains two equal-intensity resonances at δ(P) = 51.5 [^1J(PtP) = 5432 Hz, ^2J(PtP) = 231 Hz] and 38.6 [^1J(PtP) = 5476 Hz, ^2J(PtP) = 221 Hz], assigned to dppm phosphorus atoms adjacent to and remote from the $Ir(CO)_2$ group, respectively. Similarly, the ^{13}C NMR spectrum (Figure 3) of a ^{13}CO-enriched sample in the bridging carbonyl region contains two equal-intensity resonances at $\delta(^{13}C) = 221.6$ [^1J(PtC) = 676 Hz] and 224.0 [^1J(PtC) = 816 Hz], each with 1:8:18:8:1 intensities, assigned to the bridging carbonyls on the Pt_3 faces adjacent to and remote from the $Ir(CO)_2$ group, respectively. In the terminal carbonyl region, there was a single resonance at temperatures down to −40 °C, but this split into two equal-intensity resonances at −90 °C, neither showing resolved coupling to ^{195}Pt (Figure 4). Clearly, the $Ir(CO)_2$ group is in a conformation in which the two carbonyls are nonequivalent at −90 °C but rotation of the $Ir(CO)_2$ group with respect to the Pt_3 triangle occurs at higher temperature and leads to effective equivalence. Of course, further splitting of the $Pt_2(\mu$-CO) and PtP resonances would also be expected, but the chemical shift differences induced are probably small and only a general broadening of the spectra at −90 °C is observed. The IR spectrum of **9** contains both terminal [ν(CO) = 1956, 1932 cm^{-1}] and bridging carbonyl [ν(CO) = 1795, 1770 cm^{-1}] resonances as expected.

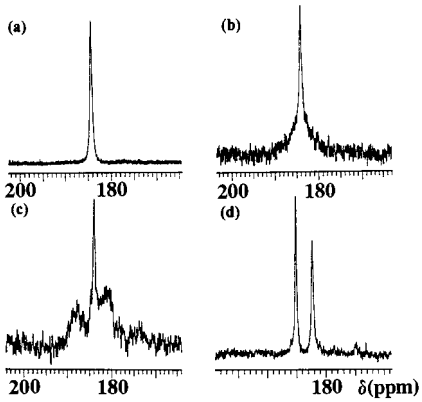

Figure 4. Variable-temperature ^{13}C NMR spectra for **9** in the region of the terminal $Ir(CO)_2$ groups: (a) 23 °C; (b) −40 °C; (c) −50 °C; (d) −90 °C.

The spectra of **10** are similar to those of **9** but there are some points of interest. The ^{31}P NMR spectrum contains three resonances with 3:3:1 intensity ratio, due to dppm phosphorus atoms adjacent to iridium, to gold, and to the Ph_3PAu group, respectively. The PAu resonance occurred at $\delta(^{31}P) = 48.9$, and appeared as a 1:4:7:4:1 multiplet due to ^2J(PtP) = 260 Hz. The ^{13}C NMR spectrum contains two equal intensity resonances in the $Pt_2(\mu$-CO) region and a terminal carbonyl resonance at $\delta(^{13}C) = 180.2$. This resonance broadened at −90 °C but did not split into two resonances; the $Ir(CO)_2$ rotation is probably easier in this case and cannot be "frozen out".

Discussion

The reactions between cluster **1** and the electrophilic reagents $[MPR_3]^+$ or InX_3 demonstrate the nucleophilic character of **1**. These reactions are analogous to those between the 42-electron triangulo clusters $[Pt_3(\mu\text{-}CO)_3(PR_3)_3]$ and $[MPR_3]^+$. Thus, the isolobal fragments $[AuPR_3]^+$, $[AgPR_3]^+$, and $[CuPR_3]^+$ possess an empty a_1' sp hybrid frontier orbital that can accept electron density from the a_1' HOMO of the clusters $[Pt_3(\mu\text{-}CO)_3(PR_3)_3]$.[2,4,13] The bonding interactions of these electrophiles with **1** will be similar since they are considered to consist of two $[Pt_3(\mu\text{-}CO)_3(PR_3)_3]$ clusters held together by the bridging dppm ligands. Naturally, the addition of ligands which do not increase the cluster electron count should not significantly affect the intertriangle Pt···Pt bonding, and the long Pt···Pt distances suggest that there is little or no Pt···Pt bonding in **5d**. The fragments $[AuPR_3]^+$ and H^+ are isolobal but they give different reactions with **1**. The reaction of H^+ with **1** is consistent with intermediate formation of a diprotonated cluster followed by fast reductive elimination of dihydrogen to give the octahedral cluster $[Pt_6(CO)_6(\mu\text{-dppm})_3]^{2+}$. In contrast, there is a more direct analogy in triplatinum clusters, for which $[Pt_3(\mu_3\text{-}AuPR_3)$-

(13) Gilmour, D. I.; Mingos, D. M. P. *J. Organomet. Chem.* **1986**, *302*, 127.

(μ-dppm)$_3$]$^+$ and [Pt$_3$(μ_3-AuPR$_3$)(μ-CO)$_3$(PCy$_3$)$_3$]$^+$ are isolobal with the corresponding hydride clusters [Pt$_3$(μ_3-H)(μ-dppm)$_3$]$^+$ and [Pt$_3$(μ_3-H)(μ-CO)$_3$(PCy$_3$)$_3$]$^+$, respectively.[14]

The reactions of cluster **1** with Hg and Tl$^+$ can be compared to analogous reactions of trinuclear platinum clusters which form 1:1 adducts, the mercury complex forming a loose dimer in the solid state through Hg−Hg bonding.[4,5] However, there are interesting differences between the reactivity of **1** and other hexanuclear platinum clusters. Thus, in [Hg$_2$Pt$_6$(μ-CNR)$_6$(μ-diphos)$_3$], [Hg$_2$Pt$_6$(μ-CNR)$_6$(CNR)$_2$(μ-diphos)$_2$] (R = 2,6-Me$_2$C$_6$H$_3$ or 2,4,6-Me$_3$C$_6$H$_2$; diphos = Ph$_2$P(CH$_2$)$_n$PPh$_2$, n = 5 or 6), [TlPt$_6$(μ-CO)$_6$(μ-dppp)$_3$]$^+$, and [HgPt$_6$(μ-CO)$_6$(μ-dppp)$_3$] (dppp = Ph$_2$P(CH$_2$)$_3$PPh$_2$), the Hg$_2$, Tl$^+$, and Hg units are trapped inside the clusters, where they are sandwiched between the two Pt$_3$ triangles.[15] The intertriangle Pt$_3$−Pt$_3$ distances in **1** are probably about 3 Å, similar to the distances found crystallographically in **5d** and in the analogous palladium cluster [Pd$_6$(μ-CO)$_6$(μ-dppm)$_3$],[16] and the cavity between the two Pt$_3$ triangles is therefore too small to accommodate a large atom like Hg. The addition to the outside faces of the cluster **1** thus occurs instead. Although Hg(0) and Tl$^+$ are formally 2-electron ligands, they appear to act as weakly electron-withdrawing ligands, perhaps by accepting more electron density by back-bonding to empty p orbitals than they donate from the filled 6s^2 orbital.

Stronger donors such as phosphites form only 1:1 adducts with **1**, and this behavior is also observed with the transition metal ligand {Ir(CO)$_2$}$^-$ in forming the 1:1 adduct **9**. The theory[8c] that strong donors transfer electron density to the remote Pt$_3$ face and thus deactivate it to attack by nucleophiles but activate it to attack by electrophiles is supported by the easy addition of {AuPR$_3$}$^+$ to **9** to give the much more stable **10**. In a sense, **10** is isolobal with the 86-electron clusters **3** and **4**, and so stronger intertriangle Pt···Pt bonding is expected compared to the cases of **5**−**8**. However, since attempts to grow X-ray-quality crystals of **9** and **10** were unsuccessful, this remains to be proved. The anionic complex **9** is really a 98-electron cluster and represents the first example of a capped trigonal prismatic cluster having this electron count.[1,2,7] The 96-electron Pt$_7$ cluster [Pt$_7$(CNXy)$_{12}$], Xy = 2,6-Me$_2$C$_6$H$_3$, has a bicapped trigonal bipyramidal core.[17]

Overall, the series of cluster complexes reported above represents the most complete set of trigonal prismatic and capped trigonal prismatic clusters yet known. The trigonal prism is favored on account of the bridging dppm ligands even when there is no intertriangle Pt−Pt bonding. Most trigonal prismatic clusters have a 90-electron count as typified by [Rh$_6$C(CO)$_{15}$]$^{2-}$ and its bicapped derivative [Rh$_6$C(CO)$_{15}$(μ_3-CuCNMe)$_2$]$^{2-}$,[17] and platinum clusters often have 4 electrons less than the simple PSEPT number, thus suggesting that 86 electrons might be the optimum electron count for trigonal prismatic hexaplatinum clusters.[7,9] In the 84- and 88-electron clusters, it is likely that there is little intertriangle Pt−Pt bonding, and this is consistent with the structure determined for **5d**.

Experimental Section

All syntheses and manipulation of materials were conducted under an inert atmosphere of dry N_2 using standard Schlenk techniques or in a Vacuum Atmospheres drybox. All glassware was flame-dried under reduced pressure and allowed to cool under dry N_2. Solvents were dried by standard methods and distilled under N_2. Infrared spectra were recorded using a Bruker IR/32 FT-IR spectrometer. NMR spectra (^{1}H, ^{13}C, and ^{31}P) were obtained using a Varian Gemini-300 MHz spectrometer, with chemical shifts (in ppm) referenced to residual solvent peaks (^{1}H and ^{13}C) or external H$_3$PO$_4$ (^{31}P). Elemental analyses were performed by Guelph Chemical Laboratories. The starting materials [Pt$_6$(μ-CO)$_6$(μ-dppm)$_3$] (**1**),[6] [Au(PR$_3$)Cl] (R = Ph, *i*Pr),[18] and [Cu(MeCN)$_4$][PF$_6$][19] were prepared according to published procedures.

[Pt$_6$(μ_3-AuPPh$_3$)$_2$(μ-CO)$_6$(μ-dppm)$_3$][PF$_6$]$_2$, 5a. Cluster **1** (0.063 g, 0.025 mmol) was dissolved in THF (20 mL). In a separate reaction vessel, [Au(PPh$_3$)Cl] (0.025 g, 0.050 mmol) and AgPF$_6$ (0.013 g, 0.050 mmol) were also dissolved in THF (10 mL), and the solution was allowed to stir for 10 min while shielded from light. This solution was then filtered over Celite into the THF solution containing **1**, leading to immediate formation of a green color. The green solution was left to stir for 1 h and was then evaporated to dryness under reduced pressure. The dark green residue was dissolved in CH_2Cl_2 (2 mL), and the product was precipitated as a green solid by addition of hexane (100 mL). Yield: 79%. Anal. Calcd for $C_{117}H_{96}Au_2F_{12}O_6P_{10}Pt_6$: C, 37.9; H, 2.6. Found: C, 37.8; H, 2.5. IR (Nujol): ν_{CO} = 1851 (s), 1816 (sh) cm^{-1}. NMR data in CD_2Cl_2 (−90 °C): δ(^{1}H) = 4.58 [s, br, C***H***$_2$ of dppm]; δ(^{13}C) = 237.9 [q, br, ^1J(PtC) = 602 Hz, μ-***C***O]; δ(^{31}P) = 42.5 [s, br, ^1J(PtP) = 5070 Hz, ^2J(PtP) = 230 Hz, μ-dppm], 88.0 [s, br, ^2J(PtP) = 281 Hz, ***P***Ph$_3$].

[Pt$_6$(μ_3-AgPPh$_3$)$_2$(μ-CO)$_6$(μ-dppm)$_3$][PF$_6$]$_2$, 5b. Cluster **1** (0.046 g, 0.019 mmol) was dissolved in THF (10 mL). In a separate flask, PPh$_3$ (0.0098 g, 0.037 mmol) and AgPF$_6$ (0.0094 g, 0.037 mmol) were treated with THF (15 mL), and the mixture was allowed to stir for 10 min while shielded from light. The THF solution containing the silver reagent was then added to the solution containing cluster **1**, causing a dark green coloration. The solution was left to stir for several minutes (shielded from light), and the solvents were evaporated under vacuum to give the product as a dark green solid. Yield: 87%. Anal. Calcd for $C_{117}H_{96}Ag_2F_{12}O_6P_{10}Pt_6$: C, 39.9; H, 2.9. Found: C, 40.3; H, 2.9. IR (Nujol): ν_{CO} = 1835 (s), 1810 (s) cm^{-1}.

[Pt$_6$(μ_3-CuPPh$_3$)$_2$(μ-CO)$_6$(μ-dppm)$_3$][PF$_6$]$_2$, 5c. Cluster **1** (0.043 g, 0.017 mmol) was dissolved in THF (20 mL). In a separate reaction vessel, [Cu(MeCN)$_4$][PF$_6$] (0.013 g, 0.034 mmol) and PPh$_3$ (0.0090 g, 0.034 mmol) were dissolved in THF (10 mL), and the mixture was allowed to stir for 10−15 min. This solution was then transferred to the THF solution containing **1**, immediately causing a green coloration. The green solution was left to stir for 15 min, and the solvent was then evaporated under vacuum. The dark green residue was recrystallized via slow diffusion of pentane (10 mL) into a CH_2Cl_2 solution (2 mL) of the product at −20 °C over 24 h. A dark green, microcrystalline powder was obtained and dried under reduced pressure. Yield: 85%. Anal. Calcd for $C_{117}H_{96}Cu_2F_{12}O_6P_{10}Pt_6$: C, 40.9; H, 2.8. Found: 40.5; H, 2.8. IR (Nujol): ν_{CO} = 1880 (sh), 1839 (s) cm^{-1}. NMR data in CD_2Cl_2 (−90 °C): δ(^{1}H) = 4.46 [s, br, C***H***$_2$ of dppm]; δ(^{13}C) = 233.2 [q, br, ^1J(PtC) = 609 Hz, μ-***C***O]; δ(^{31}P) = 44.8 [s, br, ^1J(PtP) = 5127 Hz, ^2J(PtP) = 228 Hz, μ-dppm], 52.4 [s, br, ***P***Ph$_3$].

[Pt$_6$(μ_3-AuP*i*Pr$_3$)$_2$(μ-CO)$_6$(μ-dppm)$_3$][PF$_6$]$_2$, 5d. Cluster **5d** was prepared and isolated in a manner analogous to that outlined for cluster **5a** but using [Au(P*i*Pr$_3$)Cl] in place of [AuCl(PPh$_3$)]. Yield: 94%. Anal. Calcd for $C_{99}H_{108}Au_2F_{12}O_6P_{10}Pt_6$: C, 34.0; H, 3.1. Found: C, 34.1; H, 3.0. IR (Nujol): ν_{CO} = 1875 (w), 1834 (s) cm^{-1}. NMR data in CD_2Cl_2 (−90 °C): δ(^{1}H) = 4.52 [s, br, C***H***$_2$ of dppm]; δ(^{13}C) = 237.4 [br, μ-***C***O]; δ(^{31}P) = 43.6 [s, br, ^1J(PtP) = 5047 Hz, μ-dppm], 110.9 [s, br, ***P****i*Pr$_3$].

[Pt$_6$(μ_3-InCl$_3$)$_2$(μ-CO)$_6$(μ-dppm)$_3$], 6a. To a solution of **1** (0.060 g, 0.024 mmol) in THF (25 mL) was added InCl$_3$ (0.011 g, 0.048

(14) (a) Lloyd, B. R.; Puddephatt, R. J. *J. Am. Chem. Soc.* **1985**, *107*, 7785. (b) Dahmen, K.-H.; Imhof, D.; Venanzi, L. M. *Helv. Chim. Acta* **1994**, *77*, 1029.
(15) (a) Tanase, T.; Horiuchi, T.; Yamamoto, Y. *J. Organomet. Chem.* **1992**, *440*, 1. (b) Hao, L.; Vittal, J. J.; Puddephatt, R. J. *Inorg. Chem.* **1996**, *35*, 269.
(16) Holah, D. G.; Hughes, A. N.; Krysa, E.; Magnuson, V. R. *Organometallics* **1993**, *12*, 4721.
(17) (a) Yamamoto, Y.; Aoki, K.; Yamazaki, H. *Organometallics* **1983**, *2*, 1377. (b) Albano, V. G.; Braga, D.; Martinengo, S.; Chini, P.; Sansoni, M.; Strumolo, D. *J. Chem. Soc., Dalton Trans.* **1980**, 52.
(18) McAuliffe, C. A.; Parish, R. V.; Randall, P. D. *J. Chem. Soc., Dalton Trans.* **1979**, 1730.
(19) Kubas, G. J. *Inorg. Synth.* **1990**, *28*, 90.

mmol). The reaction solution was left to stir for 1 h, after which it appeared dark yellow-brown. The solvent was evaporated under vacuum, the residue was dissolved in acetone (2 mL), and the product was precipitated as a brown solid by addition of hexane (100 mL). Yield: 88%. Anal. Calcd for $C_{81}H_{66}Cl_6In_2O_6P_6Pt_6$: C, 33.2; H, 2.3. Found: C, 33.1; H, 2.5. IR (Nujol): ν_{CO} = 1895 (sh), 1836 (vs) cm^{-1}. NMR data in $CDCl_3$ (25 °C): $\delta(^1H)$ = 4.15 [s, br, C***H***$_2$ of dppm]; $\delta(^{13}C)$ = 219.4 [q, br, ^1J(PtC) = 566 Hz, μ-***C***O]; $\delta(^{31}P)$ = 49.6 [s, br, ^1J(PtP) = 5038 Hz, μ-dppm].

[Pt$_6$(μ_3-InBr$_3$)$_2$(μ-CO)$_6$(μ-dppm)$_3$], 6b. Cluster **6b** was prepared similarly but using $InBr_3$ in place of $InCl_3$. Yield: 90%. Anal. Calcd for $C_{81}H_{66}Br_6In_2O_6P_6Pt_6$: C, 30.3; H, 2.1. Found: C, 30.0; H, 2.1. IR (Nujol): ν_{CO} = 1897 (sh), 1844 (vs) cm^{-1}. NMR data in CD_2Cl_2 (23 °C): $\delta(^1H)$ = 4.19 [s, br, ^3J(PtH) = 46 Hz, C***H***$_2$ of dppm]; $\delta(^{13}C)$ = 222.1 [q, br, ^1J(PtC) = 592 Hz, μ-***C***O]; $\delta(^{31}P)$ = 48.3 [s, br, ^1J(PtP) = 5063 Hz, μ-dppm].

[Pt$_6$(μ_3-Tl)$_2$(μ-CO)$_6$(μ-dppm)$_3$][PF$_6$]$_2$, 7. Cluster **1** (0.062 g, 0.025 mmol) and $TlPF_6$ (0.017 g, 0.050 mmol) were allowed to stir in THF (30 mL) for 1 h, giving a dark blue solution. The solvent was evaporated under vacuum, the residue was dissolved in acetone (1−2 mL), and the product was precipitated as a dark blue solid by addition of hexane (100 mL). Yield: 97%. Anal. Calcd for $C_{81}H_{66}F_{12}O_6P_8Pt_6Tl_2$: C, 30.4; H, 2.1. Found: C, 30.2; H, 1.95. IR (Nujol): ν_{CO} = 1885 (sh), 1841 (s), 1790 (sh) cm^{-1}. NMR data in $(CD_3)_2CO$ (23 °C): $\delta(^1H)$ = 4.79 [s, br, ^3J(PtH) = 52 Hz, C***H***$_2$ of dppm]; $\delta(^{13}C)$ = 235.4 [q, br, ^1J(PtC) = 733 Hz, μ-***C***O]; $\delta(^{31}P)$ = 46.0 [s, br, ^1J(PtP) = 4813 Hz, ^2J(PtP) = 287 Hz, μ-dppm].

[Pt$_6$(μ_3-Hg)$_2$(μ-CO)$_6$(μ-dppm)$_3$], 8. Cluster **1** (0.047 g, 0.019 mmol) and a drop of Hg(l) (excess) were placed in a Schlenk tube under N_2. Dry THF (10 mL) was added, and the solution was allowed to stir under N_2 for 24 h. The solution changed color from dark purple to dark blue-green. The solvent was evaporated, the residue was extracted into a solution of $C_2H_4Cl_2$/MeOH (5:1, 50 mL), and the solution was filtered through Celite to remove unreacted Hg(l) to give a blue-green filtrate. The solvent volume was reduced by evaporation under vacuum, and the product was purified by precipitation with hexane to give a deep blue-green solid. Yield: 82%. Anal. Calcd for $C_{81}H_{66}O_6P_8Hg_2Pt_6$: C, 33.6; H, 2.3. Found: C, 33.3; H, 2.6. IR (Nujol): ν_{CO} = 1843 (sh), 1811 (s) cm^{-1}. Cluster **8** was found to be very sparingly soluble in THF, CH_2Cl_2, and $C_2H_4Cl_2$, to be insoluble in C_6H_6 and toluene, and to decompose in acetone. NMR data in CD_2Cl_2 (23 °C): $\delta(^{31}P)$ = 51.2 [br, ^1J(PtP) ≈ 5600 Hz, μ-dppm].

Reaction of Cluster 8 with CH_2I_2. Cluster **8** (0.045 g, 0.0156 mmol) was dissolved in $C_2H_4Cl_2$/MeOH (5:1, 20 mL) to give a dark blue-green solution. Excess CH_2I_2 (0.5 mL) was added, and the solution was left to stir for 1 h. The resulting dark red solution was concentrated to dryness under reduced pressure to give a dark red residue. The residue, which was characterized spectroscopically as [Pt$_6$(μ_3-HgI)$_2$(μ-CO)$_6$(μ-dppm)$_3$], was dried under reduced pressure. NMR data in CD_2Cl_2 (23 °C): $\delta(^1H)$ = 4.15 [s, br, ^3J(PtH) = 48 Hz, C***H***$_2$ of dppm]; $\delta(^{31}P)$ = 52.8 [s, br, ^1J(PtP) = 5160 Hz, ^2J(PtP) = 339 Hz, μ-dppm].

[Pt$_6${μ_3-AuPPh$_3$}{μ_3-Ir(CO)$_2$}(μ-CO)$_6$(μ-dppm)$_3$], 10. THF (10 mL) was added to a mixture of cluster **1** (0.074 g, 0.030 mmol) and [PPN][Ir(CO)$_4$] (0.025 g, 0.030 mmol), and the resulting mixture was stirred at room temperature for 5 min to give a blood red solution of cluster **9**. To this solution was added a solution of $[Au(THF)(PPh_3)]^+$, freshly prepared from a mixture of [AuCl(PPh$_3$)] (0.015 g, 0.030 mmol) and $AgPF_6$ (0.0075 g, 0.030 mmol) in THF (10 mL), filtered to remove the precipitate of AgCl. The resulting solution, which immediately became dark red-brown, was evaporated under vacuum. The residue was extracted with CH_2Cl_2 (2 mL), and the solution was layered with pentane (5 mL) and cooled to −20 °C for 24 h, to give dark red-brown crystals of the product **10**. Yield: 91%. Anal. Calcd for $C_{101}H_{81}AuIrO_8P_7Pt_6$: C, 37.9; H, 2.6. Found: C, 38.2; H, 2.5. IR (Nujol): ν_{CO} = 1995 (br), 1962 (sh), 1931 (sh), 1843 (sh), 1811 (s) cm^{-1}. NMR in $(CD_3)_2CO$ (0 °C): $\delta(^1H)$ = 4.56 [C***H***$_2$P$_2$]; $\delta(^{13}C)$ = 227.0 [m, ^1J(PtC) = 676 Hz, μ-***C***O on Au-capped face], 219.7 [m, ^1J(PtC) = 754 Hz, μ-***C***O on Ir-capped face], 180.2 [br, Ir***C***O]; $\delta(^{31}P)$ = 53.5 [br, ^1J(PtP) = 5230 Hz, P of μ-dppm on Ir-capped face], 47.1 [br, ^1J(PtP^b) = 5080 Hz, P of μ-dppm on Au-capped face], 48.9 [br, ^2J(PtP) = 260 Hz, AuPPh$_3$].

Table 2. Crystal Data and Experimental Details for **5d**[a]

empirical formula	$C_{199}H_{218}Au_4Cl_4F_{12}O_{12}P_{18}Pt_{18}$
fw	6857.94
temp, wavelength	25 °C, 0.710 73 Å
cryst syst, sp gp	triclinic, $P\bar{1}$
unit cell dimens	a = 15.505(4) Å
	b = 26.544(5) Å
	c = 30.690(6) Å
	α = 91.46(1)°
	β = 96.21(1)°
	γ = 103.72(1)
volume, Z	12181(5) Å^3, 2
abs coeff, F(000)	9.476 mm^{-1}, 6412
reflns, indep reflns	27513, 25732 [R(int) = 0.0663]
data/restraints/params	13274/465/1105
goodness-of-fit on F^2	1.021
final R indices [$I > 2\sigma(I)$]	R1 = 0.0796, wR2 = 0.1838
R indices (all data)	R1 = 0.1743, wR2 = 0.2384

[a] R1 = $\sum(||F_o| - |F_c||)/\sum|F_o|$; wR2 = $[\sum w(F_o^2 - F_c^2)^2/\sum wF_o^4]^{1/2}$; GOF = $[\sum w(F_o^2 - F_c^2)^2/(n-p)]^{1/2}$, where n is the number of reflections and p is the number of parameters refined.

X-ray Structure Determination

Very dark red needles were grown from CH_2Cl_2/ether by solvent diffusion at temperature. A crystal fragment with dimensions of 0.47 × 0.18 × 0.16 mm was mounted in a Lindemann capillary tube, and the tube was flame sealed. The density was determined by the neutral buoyancy method. The diffraction experiments were carried out using a Siemens P4 diffractometer with the XSCANS software package[20] using graphite-monochromated Mo Kα radiation at 25 °C. The cell constants were obtained by centering 21 reflections (20.96 ≤ 2θ ≤ 25.04°). The Laue symmetry $\bar{1}$ was determined by merging symmetry-equivalent reflections. The data were collected in the θ range 1.5−21.0° (−1≤ h ≤ 15, −26 ≤ k ≤ 25, −30 ≤ l ≤ 30) in the ω scan mode at variable scan speeds (2−30°/min) over a period of 20 days. Background measurements were made at the ends of the scan range. Four standard reflections were monitored at the end of every 297-reflection collection. The data collection was discontinued beyond 2θ = 42° since only 20% of the reflections collected were significant in the 2θ range 38−42°. An empirical absorption correction based on the ψ scan data was applied to the data (μ = 9.476 mm^{-1}). In the triclinic system, the space group $P\bar{1}$ was assumed for Z = 2 with two independent molecules in the asymmetric unit. The data processing, solution, and F^2 refinements were done using SHELXTL programs.[21] Anisotropic thermal parameters were refined for all the platinum, gold, phosphorus, and oxygen atoms. The rest of the atoms were refined isotropically. All the phenyl rings were treated as regular hexagons with C−C = 1.390 Å. During the least-squares refinements, some methyl carbons of the 2-propyl groups showed relatively large thermal motions, but disorder was not present and the distances (C−C = 1.542 Å) and the angles (109.5°) in all the 2-propyl groups were idealized using the DFIX option. The two PF_6^- anions were found in four places in the crystal lattice where a phosphorus (P(17)) of one of the PF_6^- anions was sitting on an inversion axis. The occupancy factors for the atoms in the other PF_6^- anions were fixed at 0.5. The PF_6^- anions were treated as regular octahedrons with P−F distances of 1.600 Å. Individual isotropic thermal parameters were refined for all fluorine atoms except for F(16)−F(21), for which a common isotropic temperature factor was

(20) *XSCANS Reference Manual*, Version 2.1; Siemens Analytical X-ray Instruments Inc.: Madison, WI, 1993.
(21) *SHELXTL*, Version 5; Siemens Analytical X-ray Instruments Inc.: Madison, WI, 1994.

refined. The Fourier difference at this stage revealed the presence of a molecule of CH_2Cl_2 in two different places with occupancy factors of 0.5 each. The Cl^- ions were highly disordered, and their positions were not refined in the least-squares cycles. No attempt was made to locate the hydrogen atoms. However, all the hydrogen atoms were placed in idealized positions for the purpose of structure factor calculations only. In the final least-squares refinement cycles on F^2, the model converged at R1 = 0.0796, wR2 = 0.1838, and GOf = 1.021 for 13 274 observations with $I \geq 2\sigma(I)$ and 1105 parameters. In the final difference Fourier synthesis, the electron density fluctuated in the range +1.591 to −1.208 e Å^{-3} ; of these, the top peak was associated with the Au(2) atom. The mean and the maximum shift/esd values in the final cycles were 0.011 and 0.343. The program MISSYM[22] did not reveal any additional symmetry present in the molecule. The experimental details are given in Table 2, and complete crystal data, positional and thermal parameters, bond distances and angles, anisotropic thermal parameters, and hydrogen atom coordinates are given as Supporting Information.

Acknowledgment. We thank the NSERC (Canada) for financial support.

Supporting Information Available: An X-ray crystallographic file, in CIF format, for the structure determination of **5d** is available on the Internet only. Access information is given on any current masthead page.

IC980555J

(22) LePage, Y. *J. Appl. Crystallogr.* **1987**, *20*, 264.